Colloids and Surfaces B: Biointerfaces 82 (2011) 46–53

Contents lists available at ScienceDirect

Colloids and Surfaces B: Biointerfaces

journal homepage: www.elsevier.com/locate/colsurfb

Solubilization of fullerene C_{60} in micellar solutions of different solubilizers

Vukosava Milic Torres[a,b,*], Mihalj Posa[c], Branislava Srdjenovic[c], Ana Luísa Simplício[a]

[a] ITQB-UNL, Av. da República, Estação Agronómica Nacional, 2780-157 Oeiras, Portugal
[b] Laboratory of Proteomics, Department of Genetic, National Institute of Health Dr Ricardo Jorge, Avenida Padre Cruz, 1649-016 Lisbon, Portugal
[c] Department of Pharmacy, Medical faculty, University of Novi Sad, Hajduk Veljkova 3, 21000 Novi Sad, Serbia

ARTICLE INFO

Article history:
Received 22 April 2010
Received in revised form 2 August 2010
Accepted 6 August 2010
Available online 14 August 2010

Keywords:
Fullerene
Solubilization
Surfactants
Lipid peroxidation
Dynamic Light Scattering
Principal Component analysis

ABSTRACT

Fullerene (C_{60}), the third carbon allotrope, is a classical engineered material with the potential application in biomedicine. However, extremely high hydrophobicity of fullerene hampers its direct biomedical evaluation and application. In this work, we investigated the solubilization of fullerene using 9 different solubility enhancers: Tween 20, Tween 60, Tween 80, Triton X-100, PVP, polyoxyethylene (10) lauryl ether, n-dodecyl trimethylammonium chloride, myristyl trimethylammonium bromide and sodium dodecyl sulphate and evaluated its antioxidant activity in biorelevant media. The presence of C_{60} entrapped in surfactant micelles was confirmed by UV/VIS spectrometry. The efficacy of each modifier was evaluated by chemometric analysis using experimental data for investigating the relationship between solubilization and particle size distribution. Hierarchical clustering and principal component analysis was applied and showed that non-ionic surfactants provide better solubilization efficacy (>85%). A correlation was established ($r = 0.975$) between the degree of solubilization and the surfactant structure. This correlation may be used for prediction of C_{60} solubilization with non-tested solubility modifiers. Since the main potential biomedical applications of fullerene are based on its free radical quenching ability, we tested the antioxidant potential of fullerene micellar solutions. Lipid peroxidation tests showed that the micellar solutions of fullerene with Triton and polyoxyethylene lauryl ether kept high radical scavenging activity, comparable to that of aqueous suspension of fullerene and BHT. The results of this work provide a platform for further solubilization and testing of pristine fullerene and its hydrophobic derivatives in a biological benign environment.

1. Introduction

Fullerenes, the large carbon cage molecules considered to be three dimensional analogues of benzene, represent a third allotropic modification of carbon [1]. Fullerene C_{60}, the most representative member of this family, has the shape of an icosahedron, containing 12 pentagons and 20 hexagons, in which every carbon atom is bound to three other adjacent atoms through sp^2 hybridization [2]. Unique physical and chemical features of fullerene provide the possibility for conducting various types of chemical transformations that have resulted in wide variety of biologically active substances [3–10].

The biological activities of fullerenes are considerably influenced by their chemical modifications and light treatment [11–15]. The most relevant feature of fullerene C_{60} is the ability to act as a free radical scavenger [16]. Properties attributed to the delocalized π double bond system of fullerene cage allow C_{60} to quench various free radicals more efficiently than conventional antioxidants [10]. One of the major problems that still hamper biomedical application of fullerene is related to its extreme hydrophobicity. With solubility of less than 10^{-9} mg/L, powdered C_{60} is virtually insoluble in water. An investigation of 47 solvents has shown that the best solvents for solubilization of C_{60} have similar physical properties to the fullerenes: high refractive index, dielectric constant near 4 and large molecular volume [17]. However, organic solvents suitable for the solubilization of C_{60} are not appropriate to introduce exogenous compounds into biological systems. To overcome this problem, several approaches for the transfer fullerenes into water have been developed: chemical modification of the fullerene carbon cage, incorporation of fullerenes into water soluble supramolecular structures using surfactants, solvent exchange and long term stirring of pure C_{60} in water. Attachment of various functional groups on the fullerene core can change the photophysical properties and ROS (reactive oxygen species) quenching capacity of C_{60}, and it does not always warrant water solubility. Solvent exchange has been the most common strategy to produce stable dispersion of fullerene in water without any stabilizing agent. Scrivens and Tour dissolved C_{60} in benzene, diluted it with

* Corresponding author at: Laboratory of Proteomics, Department of Genetic, National Institute of Health Dr Ricardo Jorge, Avenida Padre Cruz, 1649-016 Lisbon, Portugal. Tel.: +351 96 15 53 682.
E-mail address: djwukie@gmail.com (V.M. Torres).

0927-7765/$ – see front matter © 2010 Elsevier B.V. All rights reserved.
doi:10.1016/j.colsurfb.2010.08.012

tetrahydrofuran (THF), then with acetone, and finally with water [12]. One of the ways to obtain stable suspensions of C_{60} is to sonicate a mixture of a toluene/water solution of fullerene, several hours using ultrasonic bath, until toluene is completely evaporated [13–15]. Deguchi et al. obtained stable dispersions of fullerene as fine clusters only using THF and water. Unfortunately, water suspension obtained by this method reached concentration of C_{60} of only around 10 μM [16].

Different solubility enhancers have been added to form supramolecular fullerene nanoparticles. γ-Cyclodextrin has been shown to form non-covalent supramolecular 2:1 host–guest complex with fullerene, which in aqueous solution, exists in a monomeric state, possibly due to the formation of hydrogen bonds [18,19]. Benesasson et al. demonstrated that C_{60} is extensively incorporated into phosphatidylcholine liposomes, but the degree of aggregation depends mainly on the relative concentration of C_{60} to phosphatidylcholine [20]. These findings open the possibility for transferring individual molecules of fullerene to biological cells via liposome interaction with cell membrane. Other macromolecules such as calixarene [21], polyvinylpyrrolidone (PVP) [22–24], lecithin [25] have been used to prepare water stable C_{60} aggregates. Surfactant solutions also offer a versatile solubilization method, since the micellar environment is chemically inert towards fullerenes. Surfactants, as a Triton X-100 (TX100) or the Tween group, are known to form spherical micelles at the critical micellar concentration (CMC). According to previous findings, spherical micelles of these surfactants are ideal candidates for entrapping fullerene and preparing stable homogenous dispersions [20,26–29].

According to our knowledge, work on solubilization of C_{60} has been done mainly with individual surfactants but there is no comparative data on the solubilization efficacy of fullerene with different surfactants, and determination of its antioxidant capacity in aqueous solutions. In the present work, we have tested a set of nine surfactants to solubilize pristine C_{60}, and obtained a detailed insight on the formation of supramolecular structures, and solubility ability of each micellar fullerene/surfactant system.

Additionally, this work provides an explanation for the differences observed in fullerene solubilization in micellar solutions, considering the structures of the surfactants used. Chemometric analysis allowed obtaining correlations between the degree of solubilization (SCMC [%]) and the structure of the detergent, which can serve for future prediction of solubilization efficacy of non-tested surfactants.

We have also tested the antioxidant potential (TBARS) of all solubilized forms of C_{60} in a biological friendly environment and compared it with the activity of butylated hydroxytoluene (BHT). This data provides an insight into the most promising solubilizers for future biomedical applications of fullerene and fullerene hydrophobic derivatives.

2. Materials and methods

2.1. Chemicals

C_{60} 99.5% purity was purchased from MER Corp., Arizona. Toluene and hexane, both spectroscopy grade, polyoxyethylene (10) lauryl ether ($C_{12}E_{10}$), n-dodecyl trimethylammonium chloride (DTAC), myristyl trimethylammonium bromide (MTAB) and polyvinylpyrrolidone (PVP) Mw ~ 40,000, Triton X-100 (TX100) were from Sigma–Aldrich. Tween 20 (T20), Tween 60 (T60), Tween 80 (T80) and sodium dodecyl sulphate (SDS) were from Fluka. Ultrapure water (surface tension—7.19×10^{-2} J/m^2; resistivity—18.2 MΩ cm @ 25 °C), produced by a Millipore Elix A3-MilliQ system (MilliQ, Germany), was used for preparation of aqueous solutions.

2.2. Encapsulation of C_{60} into micellar solutions

Neat TX100, T20, T60, T80, $C_{12}E_{10}$, SDS, DTAC or MTAB was added to 2 mL of C_{60}-toluene solution (27.5 μM). Exception was made with the PVP solution, which was previously dissolved in $CHCl_3$ (2 mL), and then added to 1 mL of toluene containing 50 μL of stock solution C_{60} (1.1 mM). For solubility tests, concentration of solubility enhancers was subsequently increased from 0.25 to 1200 cmc. Prepared solutions were mixed overnight using a magnetic stirrer (500 r/min), and after, gently evaporated, at 50 °C, under the stream of nitrogen, until residues of solvents were removed. The residue was dissolved in 2 mL of water, and filtered through 0.45 μm, 13 mm diameter Nylon puradisc syringe filters (Whatman). Samples were stored at room temperature, protected from light.

2.3. Preparation of aqueous suspensions of C_{60}

Each stable suspension of fullerene was prepared by solvent exchange process with toluene and water [13]. 1 mL of toluene solution containing 55 nmol of C_{60} (50 μL of fullerene stock solution) was added to 2 mL of water, and the mixture was sonicated for approximately 5 h until the evaporation of toluene was complete. The aqueous solution was filtered through 0.45 μm Nylon syringe filters resulting in clear, transparent, brownish-yellow colored solution. The solution was stored at room temperature, protected from light.

2.4. Particle size determination

For particle size determination, a Malvern Instruments Zeta-Sizer Nano ZS (Malvern Instruments, Worcestershire, UK) was used. The ZetaSizer is a dynamic light scattering device that determines particle size from measured diffusion coefficient, using the Stokes–Einstein equation ($Rh = kT/6\pi\eta D$). Intensity of particle size distribution was measured by 173° backscatter detection (NIBS).

2.5. Characterisation and determination of C_{60} concentration in micellar solution

Electronic absorption spectra were recorded on a double beam spectrophotometer UV/VIS Shimadzu 1630, using a quartz cell with 1 cm path length. Concentrations of C_{60} in micellar solutions were initially determined by the Beer's law, using an empirically derived molar absorption coefficient of $\log \varepsilon$ 4.717 at λ_{max} 330 nm in n-hexane [20,27]. For that purpose micelles were destroyed by adding KCl and toluene. After sonication, mixture was kept at room temperature, protected from the light overnight and centrifuged. The toluene layer was carefully withdrawn and used for spectrophotometric measurement. Efficacy of extraction was over 90%.

Direct readings from aqueous solutions using the same absorption coefficient afforded equivalent results, and therefore were used it for further determinations.

2.6. TBARS assay

2.6.1. Thiobarbituric acid reactive substances (TBARS) assay

The antioxidant properties of micellar fullerene solutions were determined by inhibition of lipid peroxidation. For this measurement, the modified method of Uchiama and Mihara was used for determining TBARS in the reaction mixture [30]. Briefly the reaction mixture containing 30 μL of corn oil containing Tween (0.05 g Tween 80 in 10 g cold pressed corn oil), 10 μL of sample, water or BHT solution, 125 μL H_2O_2 30% (Panreac, Spain), 125 μL of $FeSO_4$ (Sigma–Aldrich, USA) 9 mM in 3 mL 1% H_3PO_4 (JT Baker, USA) was incubated 1 h at 37 °C. After cooling, 1 mL of 0.6% thiobarbituric

acid (TBA) (Sigma–Aldrich, USA) was added, mixed and incubated again for 45 min at 90 °C. After cooling, extraction was carried out with 3 mL of 2-butanol (Poch, Czech Republic) and the organic layer was separated by centrifugation. The optical density of the organic layer was determined by UV/VIS spectrophotometry at 535 nm, $\varepsilon = 1.56 \times 10^5\ M^{-1}\ cm^3$. The TBARS level was expressed as % of nmol/mL of oil related to control

2.6.2. Chemometric measurements

Molecular descriptors for solubility enhancers were obtained using the program package Chem3DUltra 7.0, and the results were treated using SPSS 10.0 package for Windows, which was also used for the principal component analysis (PCA) and hierarchical classification. The protocol for comparing experimental parameters was as follows: for each parameter was constructed a dendrogram (hierarchical method of grouping of surfactant molecules with centroid linking, the measure of the distance being the square of the Euclid length in the multidimensional space) [31]. In a dendrogram, a common group was formed by the molecules whose mutual similarity exceeds 80% (strong connection) and 60% (weak connection). Then, the distribution of surfactants per groups was determined for each dendrogram by determining the percentage of distribution overlapping (the similar surfactants belong to the same group).

3. Results and discussion

3.1. Micellar solubilization of C_{60}—localization in the micellar phase

C_{60} was solubilized in aqueous solution using different solubilizers according to the procedures described in Section 2. The UV–VIS spectrum of C_{60} in toluene contains a characteristic band at 335 nm and small sharp peak at 407 nm [25,20]. In order to evaluate micellar solubilization of fullerene (27.5 μM) and its dependence on a solubilizer concentration, we monitored the absorption spectra of every prepared micellar solution of fullerene in the region from 300 to 600 nm, with special regards on its characteristic band at 335 nm and vibronic structure in the range of 400–410 nm.

Using solubility enhancers, the highest enrichment of water solution in fullerene (>85%) was achieved using: T20, T80, TX100, $C_{12}E_{10}$ and MTAB, while moderate efficacy had PVP and DTAC (~70 and 50%, respectively). The lowest solubilization power was expressed SDS (~20%) (Fig. 1).

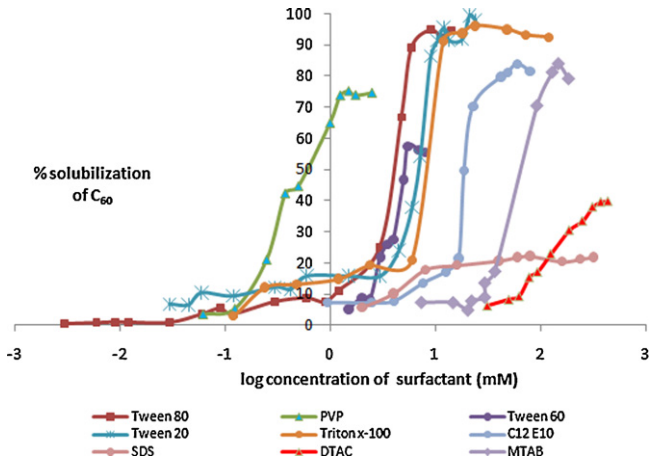

Fig. 1. Efficacy of fullerene (27 μM) solubilization depending on the surfactant.

The UV/VIS spectrum of the solutions with high content of solubilized fullerene was equivalent to that of the parent C_{60}-toluene solution (Fig. 2a). In these spectra, the characteristic band at 335 nm showed a blue shift to 330 nm, while the band at 407 nm slightly shifted to 405 nm. The weak visible band at about 540 nm, which is responsible for the purple color of toluene C_{60} solution, also shifted to lower wavelengths and influenced by stronger UV band. These findings are confirmed by a solution color change from purple to brownish-yellow. These spectral findings exhibit the characteristic features of C_{60} indicating that fullerene is located in the inner, hydrophobic part of the micelle.

The spectrums of C_{60aq}, C_{60}-PVP and C_{60}-SDS were slightly different and showed red shifts from 335 to 339 nm. These bands were also broader and less intense than corresponding bands in C_{60}-toluene solutions (Fig. 2b). The sharp peak at 407 nm disappeared and a broad band appeared at about 450 nm, indicating formation of fullerene aggregates. Deguchi et al. found similar spectral behaviour for water suspension of C_{60} and suggested that fullerene is dispersed in water as fine solid clusters [16]. Although Eastoe et al. found that ionic surfactants (SDS, CTAB) were not effective for solubilization of fullerene [26], in our experiment, SDS enhanced the solubility of fullerene in water, but with less efficacy than other used surfactants. This lack of efficacy is probably due to SDS ionic nature. We hypothesise that SDS partly makes micelles with fullerene, entrapping it into hydrophobic part of micelle, and partly

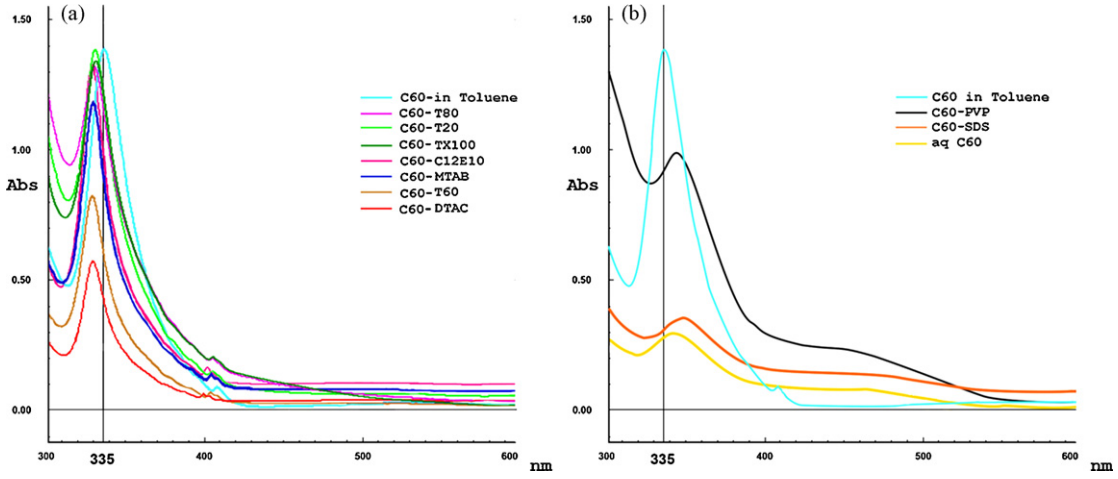

Fig. 2. Comparative UV/VIS spectra of fullerene micellar solutions related to the spectra of parent C_{60} in toluene: (a) blue shift (C_{60}-T20, C_{60}-T60, C_{60}-T80, C_{60}-TX100, C_{60}-$C_{12}E_{10}$, C_{60}-DTAC, C_{60}-MTAB); (b) red shift (C_{60}-SDS, C_{60}-PVP, aq C_{60}). (For interpretation of the references to color in this figure legend, the reader is referred to the web version of the article).

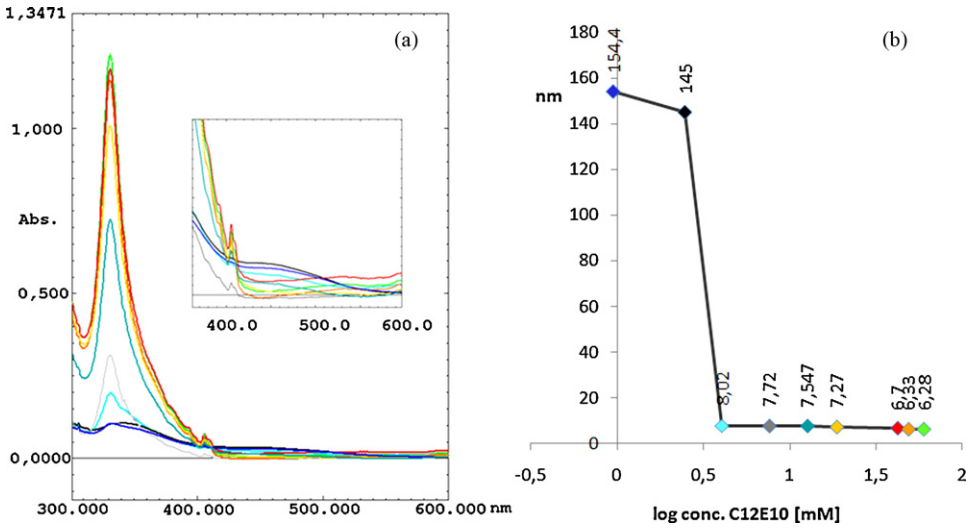

Fig. 3. UV/VIS spectra (a) and particle size distribution by DLS (b) of solubilized C_{60} (27 μM) with subsequent increase of surfactant concentration (example for $C_{12}E_{10}$: (◆) 0.9 mM; (♦) 2.5 mM; (◇) 4.0 mM; (◈) 7.5 mM; (◈) 12.5 mM; (◇) 18.5 mM; (◆) 40.2 mM; (◇) 50.0 mM; (◇) 60.10 mM).

stabilize the negatively charged surface of fullerene clusters by electrostatic repulsion between negatively charged surfaces of C_{60} aggregates and polar heads of SDS.

Results of DLS analysis confirmed spectroscopic data. After reaching the maximum solubility of fullerene, particle size was between 6 and 9 nm with exception of C_{60}-SDS and C_{60aq}. The hydrodynamic volume diameter of C_{60}-SDS and C_{60aq} was 79 and 58 nm, respectively. Eastoe et al. reported size of 10 nm for polydisperse clusters of fullerene [26], while Deguchi et al. obtained fullerene aggregates in aqueous suspension with hydrodynamic diameter of 62.8 nm [16]. Larger particle size suggests the formation of aggregates, which was additionally confirmed by the appearance of broad absorption band at 450 nm. It is important to notice that, as the concentration of surfactant increases, solubility of fullerene increases as well (Fig. 3a), while particle size decreases (Fig. 3b). It can be also observed that, when maximum solubility is reached, the broad band on 450 nm disappears while the peak at 335 shifts to 330 nm, originating the characteristic spectra of C_{60}-toluene solution.

These observations indicate that, when the solubility of fullerene is greater than 90%, solvent–solute, and solute–solute interactions are similar to the ones obtained in toluene or hexane, implying that, after an optimal supramolecular structure is obtained, fullerene is not agglomerated. Such conclusion is supported by corresponding findings in Langmuir–Blogett films of fullerene in phenolic aqueous solution of vapour deposition films of C_{60} on polar solid material [32], as well as by the work of Hungerbüehler et al. [25].

3.2. Antioxidant capacity of C_{60} micellar solutions (TBARS assay)

We studied antioxidant activities of the prepared series of water soluble forms of fullerene C_{60} by measuring the product of lipid peroxidation (LP)—thiobarbituric acid reactive substance (TBARS). Aqueous solutions of the fullerene supramolecular forms were investigated in the concentration range from 0.1 to 10 μM. Butylated hydroxytoluene (BHT) as a commercial, well known antioxidant, served as reference. Results obtained in this investigation show that the antioxidant potential strongly depends on the type of solubility enhancer, and the LP level, at all investigated supramolecular structures, varied in a concentration dependent manner. The best antioxidant activity was exhibited by stable water suspension of fullerene (C_{60aq}), which decreased the level of TBARS by more than 80% at 4.68 μM (Fig. 4). This result shows that C_{60} is more potent ROS scavenger than BHT. Our findings are in agreement with results of Wang et al. which found that liposoluble C_{60} had greater antioxidant power than vitamin E [33]. Introducing a surfactant to modify fullerene solubility caused a slight or a complete discrepancy of ROS-scavenging potentiality. In our model system, fullerene coated with ionic surfactants- MTAB, DTAC and SDS showed a prooxidative effect and supramolecular structures of C_{60} with surfactants of the Tween group (T20, T60 and T80) also exhibited the same.

On the other hand, in Fig. 4 it can be seen that C_{60}-PVP, in the same concentration range, suppresses lipid peroxidation similarly to BHT. Takada et al. reported significant inhibitory effect of PVP entrapped fullerene on the oxidative discoloration of β-carotene [23], while Xiao et al. have shown that the same supramolecular structure diminished the ROS amounts in the terms of the molecu-

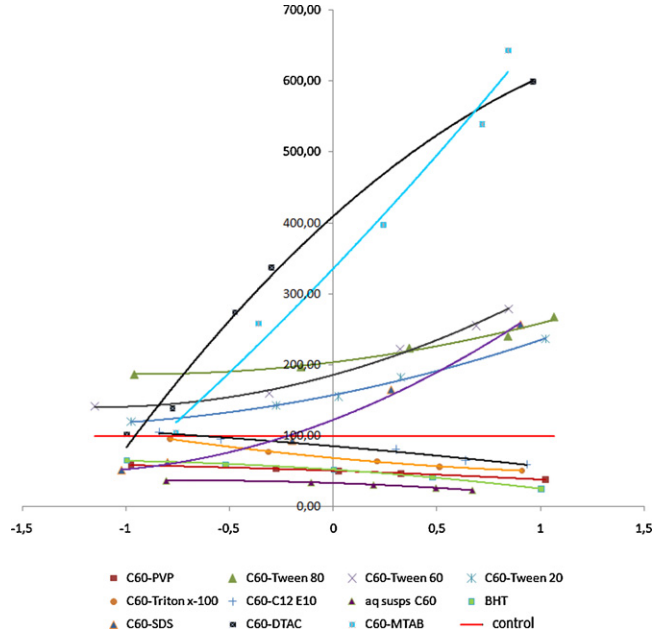

Fig. 4. Influence of supramolecular structures of fullerene (C_{60}-T20, C_{60}-T60, C_{60}-T80, C_{60}-TX100, C_{60}-$C_{12}E_{10}$, C_{60}-PVP, C_{60}-MTAB, C_{60}-DTAC, C_{60}-SDS), C_{60aq} and BHT on TBARS levels. Formation of TBARS is expressed as a percentage related to control.

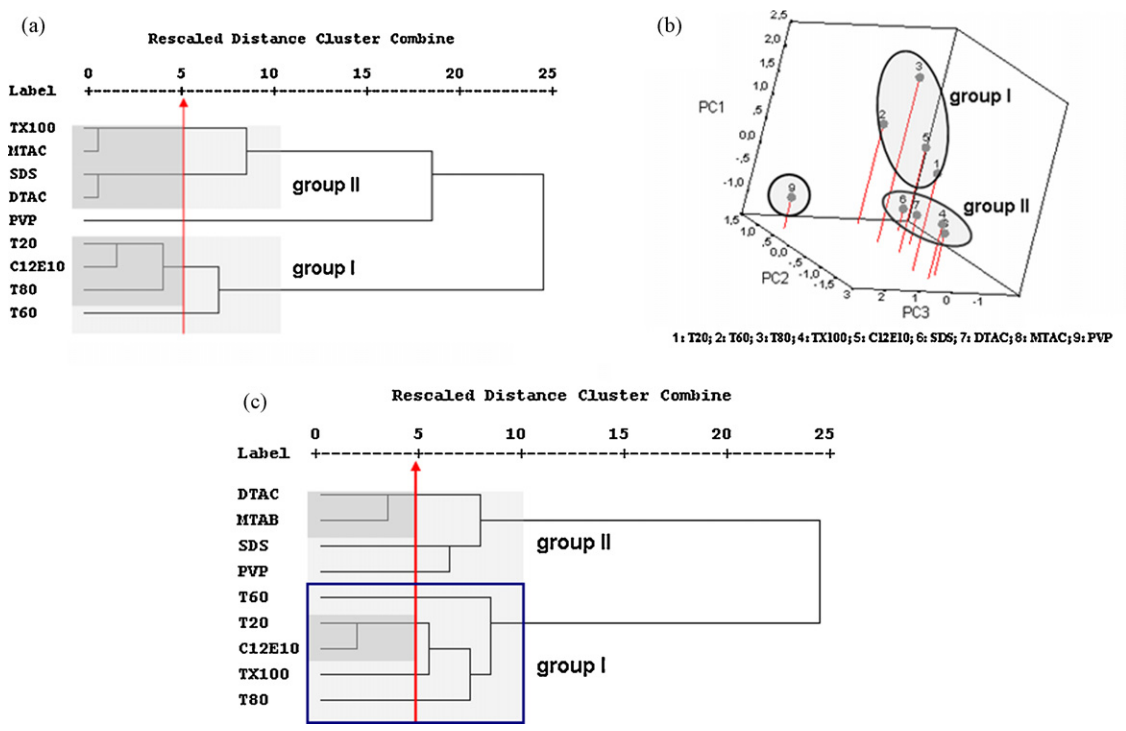

Fig. 5. Hierarchical clustering and principal component analysis (PCA) of solubilization experiment: (a) hierarchical clustering for solubilization of fullerene using solubility data; (b) grouping of detergents in PC1–PC2–PC3 space; (c) hierarchical clustering of solubilized fullerene using values of particle size distribution obtained by dynamic light scattering.

lar and cellular levels against UVB and tert-butyl hydroperoxide at concentrations of 200 and 400 μM [34].

Fullerene coated with $C_{12}E_{10}$ and TX100 demonstrated high antioxidative efficacy, decreasing the TBARS for more than 50% related to control at concentration of 8.60 and 8.14 μM, respectively.

3.3. Chemometric analysis in the space of experimental data

The relationship between solubilization and size distribution of micellar dispersed fullerene was evaluated from the obtained experimental data. Linear correlation afforded values of Pearson's coefficient between 0.5 and 0.8 (depending on the surfactant) which means that using this correlation it is not possible to determine the dependence between solubilization and particle size distribution. Therefore a hierarchical clustering method of analysis had to be used to obtain dendograms for comparison of the degree of surfactant clusters overlapping.

According to the matrices of solubilization of fullerene C_{60}, the hierarchical clustering method of analysis was applied using Euclid the distance and centroid grouping for all used concentration of analysed surfactants (Fig. 5a). Two clusters (groups) can be identified in the dendogram. This grouping was confirmed by principal component analysis (PCA). Obtained scores of principal components PC1, PC2 and PC3 explained 98.9% of total variance in the solubilization matrices of fullerene. In the PC1–PC2–PC3 space, the investigated detergents form two groups and one solubilizer (PVP) is an outlier (Fig. 5b).

The first group contains only non-ionic surfactants: T20, T60, T80 and $C_{12}E_{10}$, where T20, T80 and $C_{12}E_{10}$ are the most similar to each other (Fig. 5b). $\Delta S/\Delta c^*$ values were between 13.73 and 38.46 (average 23.07). The second group contains the ionic surfactants—DTAC, SDS, MTAB and one non-ionic (TX100) and it clearly distinguishes two subgroups of surfactants. $\Delta S/\Delta c$ values were between 0.12 and 11.73 (3.72 in average).

The dendogram constructed for DLS (Fig. 5c) revealed two groups of surfactants as in Fig. 5a. The first group contains all non-ionic detergents (T20, $C_{12}E_{10}$, TX100, T80 and T60), while the second group contains all ionic surfactants (MTAB, DTAC, SDS) and PVP. The main characteristic of group I is the upper extreme point on the curves of distribution size i.e. difference between first and last point is greater than 90 nm. Group II does not have such an extreme point and the difference between the first and last points is up to 33 nm (Table 1).

The overlapping of the detergent distribution into groups according to the size distribution (Fig. 5c) with the grouping according to solubilization is 77.5% (Fig. 5a). These results confirm the importance of size distribution in the solubilization of fullerene. In both experiments, group I was characterised by sudden change in the corresponding curves (Fig. 1). However, comparing data for particle size distribution and % of solubilization, for the same surfactant, a sudden change in particle size distribution curve occurs at lower concentration of detergent than the corresponding change in the solubilization curve. This is particularly pronounced in the first group.

This delayed "jump" in solubilization, in relation to the particle size distribution curve, probably occurs due to the specific mechanism of solubilization. Namely, when the concentration of surfactant is small, fullerene forms aggregates of larger dimensions (Fig. 6I). With increasing surfactant concentration, its molecules penetrate into the existing aggregates, in order to more effectively cover the hydrophobic surface of fullerene (Fig. 6II–IV, Fig. 7a). According to Tanford, at the low surfactant/compound ratio, water molecules penetrate the hydrophobic part of the mixed micelle, destabilizing the system and micelles break up into smaller aggregates with bigger contact surface of fullerene and water [35]. When fullerene surface is covered, further addition of surfactant is spent on "effective dissolution". Molecules are building new micelles increasing the degree of fullerene solubilization (Fig. 6V). This is manifested

Table 1
Particle size (nm) at the first and the last solubilization point, measured by DLS.

	T20	T60	T80	TX100	$C_{12}E_{10}$	PVP	DTAC	MTAB	SDS
First point of solubilization (nm)	148.0	97.6	180.5	168.7	154.4	8.9	<1.0	1.23	122.4
Last point of solubilization (nm)	5.9	6.7	7.6	7.5	6.3	6.2	<1.0	<1.0	79.1

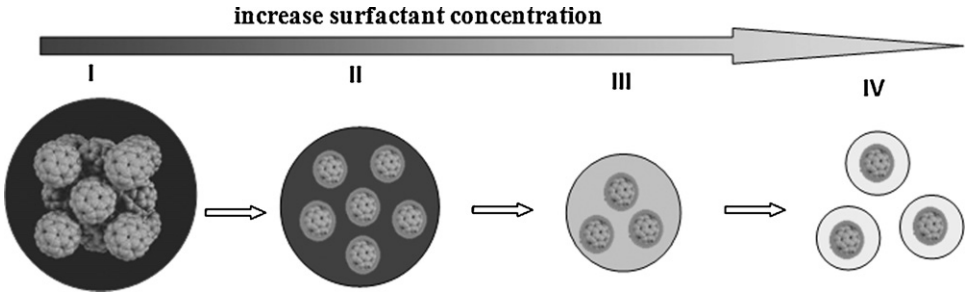

Fig. 6. Supposed mechanism of C_{60} solubilization.

by the sudden increase in the slope of the solubilization curve (Fig. 7b).

The following linear equation relates the degree of solubilization of fullerene at the cmc (S_{CMC} [%]) of each surfactant with the detergent structure:

$$S_{CMC} = 0.097 + 1.093W_{l/b} \quad (1)$$

$$n = 7; \quad r = 0.975; \quad sd = 2.34; \quad F = 20.52$$

where is $W_{l/b}$ represents the ratio between Wiener's index for the hydrophilic part and for the hydrophobic part of the surfactant. However, it is not possible to precisely define the Wiener's index for PVP (polymer with large molecular weight) and SDS because of the presence of a heteroatom (*S*). Eq. (1) best describes non-ionic surfactants. Knowing the $W_{l/b}$ is possible to predict degree of solubilization at cmc for non-tested surfactants.

Increased $W_{l/b}$ ratio (Table 2) suggests that the large and flexible poly –O–CH_2CH_2–O– string of the hydrophilic head of a non-ionic surfactant, covers the hydrophobic part of the micelle leading to the stabilization of the system. These strings (which are proton acceptors) form hydrogen bonds with molecules of water settled

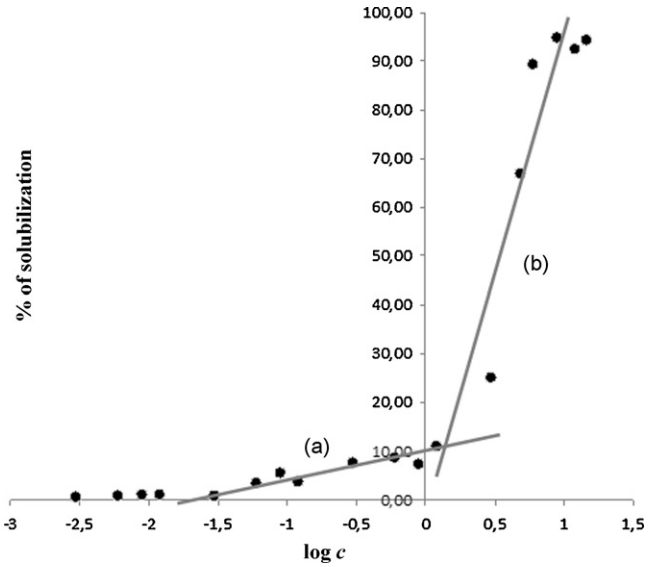

Fig. 7. Example of solubilization of fullerene with Tween 80.

Table 2
$W_{l/b}$ for tested surfactants.

$C_{12}E_{10}$	Triton X-100	Tween 20	Tween 60	Tween 80	MTAB	DTAC
16.39	12.3	6.99	1.88	1.88	0.04	0.03

in the fjords of hydrophobic parts which compensate the negative entropy resulting from hydrophobic surface hydration.

If we compare the dendogram based on hierarchical clustering for lipid peroxidation (LP) (Fig. 8) with the two previous dendograms, it can be concluded that there may be other factors which determine a different distribution of surfactants in the LP dendogram. Derivatives of Tween and SDS belong to the same group. These surfactants decreased the antioxidant activity of fullerene which can be explained by the specific structure of detergents. Namely, the big polar heads of polyosorbates of the Tween group are situated on the outer surface of the micelle and therefore prevent diffusion of Fe^{3+} and hydroxyl ($OH^{\bullet}$) radical to the C_{60} contained in its interior. At the outer surface of SDS, negative charge is delocalized across the relatively big ionic sulphate head, which easily adsorbs Fe^{3+} as a counter ion, changing the charge of the micelle to positive. The hydroxyl anion (OH^-), resulting from the Fenton's reaction, is concentrated in the diffuse layer of the micelle, stabilizing the system. Cationic surfactants (DTAC and MTAB) behaved similarly, adsorbing OH^- as a counter ion.

Fig. 9a suggests that the phenolic oxygen of Triton aromatic nucleus, with its negative inductive effect, slightly polarizes the phenyl group establishing aromatic dipole- induced dipole interactions of π electrons between the phenyl dipole and the surface

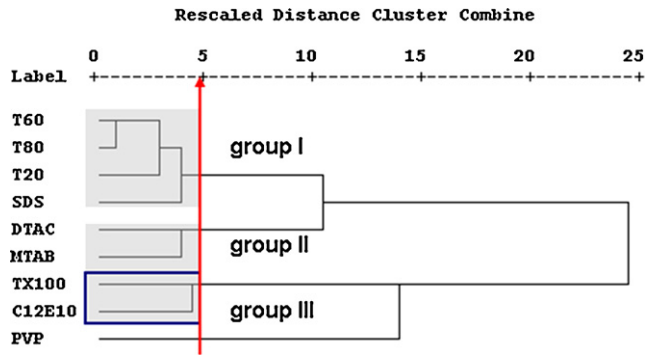

Fig. 8. Hierarchical clustering using values of lipid peroxidation experiment.

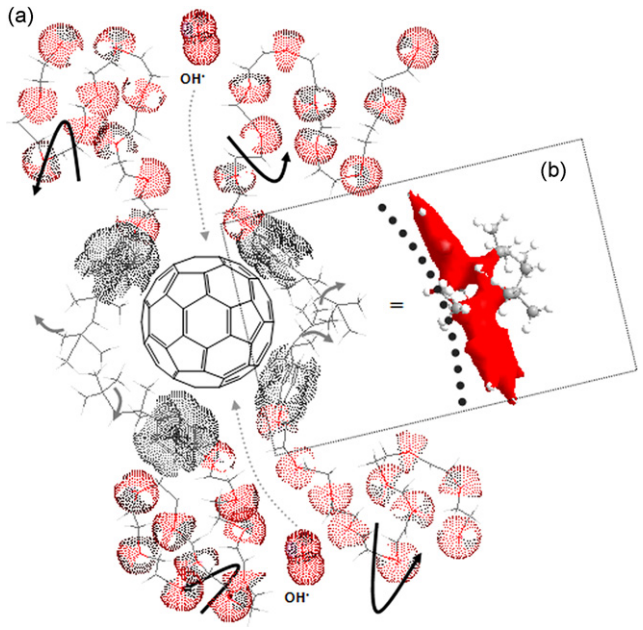

Fig. 9. (a) Hypothetical intersection of mixed micelle of Triton X-100 and C_{60}; (b) hydrophobic surface of Triton molecule through which is it in interaction with surface of fullerene as well as with vicinal molecules of surfactant.

of fullerene. The Triton molecule contains an aromatic nucleus and hydrophobic highly methylated 1,1,3,3-tetramethylbutyl chain and hydrophilic polyethoxylate string. The hydrophobic chain has relatively high degree of freedom since it contains sp^3-hybridized carbons which allow free rotation around π bonds. However, to establish the optimal interaction between Triton and fullerene (biggest surface of interaction) 1,1,3,3-tetramethylbutyl parts need to be oriented to the outer side of the micelle, since this orientation permits aromatic interaction between fullerene and phenyl part of the surfactant. Additionally, vicinal Triton molecules can be bonded via hydrophobic 1,1,3,3-tetramethylbutyl groups (Fig. 9b). Therefore, the fullerene particles are surrounded by clusters of Triton molecules in such manner that fullerene surface is only partly covered by aromatic core of surfactant. The other part of the surface is covered with flexible hydrophilic polyethoxylate strings. This large conformational flexibility of Triton polar "tails" enables diffusion of ROS to the fullerene core letting micelar solution of fullerene to exert its ROS-scavenging ability.

By analysing the dendograms, it can be concluded that PVP has the smallest similarity with the rest of the examined surfactants. It can be seen from Fig. 5a and b that PVP is isolated, not belonging to any group, while in clustering analysis related to particle size distribution (Fig. 5c), PVP is weakly connected to the second group. This could be explained by the specific properties of PVP, as a polymer with large molecular weight. It is possible that, polymeric surfactants with large molecular weight, form micellar particles with only one molecule (twisted, zigzag or globular conformation), while other investigated surfactants build associated micelles.

4. Conclusions

In this work we succeed to obtain water soluble forms of fullerene C_{60}, by solubilization with 9 different surfactants. Solubilization procedure is simple versatile and reproducible. Results of UV/VIS spectroscopy confirmed presence of fullerene in micellar particles. In the solubilization study, non-ionic surfactants showed the highest efficacy on fullerene solubilization (>85%). Ionic surfactants had lower solubilization power, with formation of aggregates, as confirmed by UV/VIS and DLS. Hierarchical clustering analysis and principal component analysis followed experimental findings. It is clearly seen that non-ionic surfactants have better solubility power, especially detergents from Tween group (T20, T60, T80) and $C_{12}E_{10}$. The linear equation obtained for solubilization of fullerene had a correlation coefficient of 0.975 and can be used for prediction of fullerene solubilization with non-tested surfactants.

Lipid peroxidation tests demonstrated that micellar solutions of fullerene with ionic surfactants (SDS, MTAB, DTAC) and surfactants from the Tween group (T20, T60, T80) hampered antioxidative properties of C_{60}. On the other hand, micellar solutions with $C_{12}E_{10}$ and Triton X-100 allowed keeping its radical scavenging properties of fullerene, which was comparable to the antioxidative activity of BHT and C_{60aq}. Hierarchical clustering analysis confirmed the experimental results. Micellar solution of C_{60} with PVP was evidenced as an outlier according to clustering analysis, although its solubilization power is moderate and ROS quenching is maintained. In conclusion- micellar solutions of fullerene with $C_{12}E_{10}$, Triton X-100 is most promising for using C_{60} in aqueous environment. Results this solubilization study allowed overcoming of hydrophobicity of C_{60} and studying fullerene antioxidant properties in a biological friendly environment, and it provides a contribution for further biomedical and pharmaceutical investigation of fullerene and its derivatives.

Acknowledgements

This work is supported by the Fundação para a Ciência e Tecnologia, Portugal, Grant No. SFRH/BPD/43365/2008.

References

[1] H.W. Kroto, J.R. Heath, S.C. O'Brein, R.F. Curl, R.E. Smalley, Nature 318 (1985) 162.
[2] W. Kratschmer, L.D. Lamb, K. Fostiropoulos, D.R. Huffman, Nature 347 (1990) 354.
[3] S. Bossi, T. Da Ros, G. Spalluto, M. Prato, Eur. J. Med. Chem. 38 (2003) 913.
[4] S.H. Friedman, D.L. DeCamp, R.P. Siibesma, G. Srdanov, F. Wudl, G.L. Kenyon, J. Am. Chem. Soc. 115 (1993) 6506.
[5] A. Isakovic, Z. Marković, B. Todorović-Marković, N. Nikolić, S. Vranješ-Đurić, M. Mirković, M. Dramicanin, Lj. Harhaji, N. Raičević, Z. Nikolić, V. Trajkovic, Toxicol. Sci. 91 (2006) 173.
[6] R. Injac, M. Perse, N. Obermajer, V. Djordjevic-Milic, M. Prijatelj, A. Djordjevic, A. Cerar, B. Strukelj, Biomaterials 29 (2008) 3451.
[7] F. Cheng, X. Yang, C. Fan, H. Zhu, Tetrahedron 57 (2001) 7331.
[8] A. Djordjevic, G. Bogdanovic, S. Dobric, J. BUON 11 (2006) 391.
[9] F. Cataldo, T. da Ros (Eds.), Medicinal Chemistry and Pharmacological Potential of Fullerenes and Carbon Nanotubes, Springer Science + Business Media B.V., 2008.
[10] P.J. Krusic, E. Wasserman, P.N. Keizer, J.R. Morton, K.F. Preston, Science 254 (1991) 1183.
[11] D. Williams, Biomaterials 29 (2008) 1737.
[12] W.A. Scrievens, J.M. Tour, J. Am. Chem. Soc. 116 (1994) 4517.
[13] G.V. Andrievsky, M.V. Kosevich, O.M. Vovk, V.S. Shelakovsky, L.A. Vashchenko, J. Chem. Soc., Chem. Commun. (1995) 1281.
[14] N.O. Mchedlov Petrossyan, V.K. Klochov, G.V. Andrievsky, J. Chem. Soc., Faraday Trans. 93 (1997) 4343.
[15] Y. Prilutski, S. Durov, L. Bulavin, P. Valerij, Y. Astashkin, V. Yashchuk, T. OgulChanski, E. Buzaneva, G. Andrievsky, Mol. Cryst. Liq. Cryst. 324 (1998) 65.
[16] S. Deguchi, R.G. Alargova, K. Tsujii, Langmuir 17 (2001) 6013.
[17] R.S. Ruof, D.S. Tse, R. Malhotra, D.C.J. Lorents, J. Phys. Chem. 97 (1993) 3379.
[18] T. Anderson, K. Nilsson, M. Sundahl, G. Westman, O. Wennerström, J. Chem. Soc., Chem. Commun. (1992) 604.
[19] B. Zhao, Y.Y. He, P.J. Bliski, C.F. Chignell, Chem. Res. Toxicol. 21 (2008) 1056.
[20] R.V. Bensasson, E. Bienvenue, M. Dellinger, S. Leach, P. Seta, J. Phys. Chem. 98 (1994) 3492.
[21] T. Haino, M. Yanase, C. Fukuanga, Y. Fukazawa, Tetrahedron 62 (2006) 2025.
[22] D.Y. Lyon, L.K. Adams, J.C. Falkner, P.J.J. Alvares, Environ. Sci. Technol. 40 (2006) 4360.
[23] H. Takada, K. Kokubo, K. Matsubayashi, T. Oshima, Biosci. Biotechnol. Biochem. 70 (2006) 3088.
[24] Y.N. Yamakoshi, T. Yagami, K. Fukuhara, S. Suyeoshi, N. Miyata, J. Chem. Soc., Chem. Commun. (1994) 517.
[25] H. Hungerbüehler, D.M. Guldi, D. Asmus, J. Am. Chem. Soc. 115 (1993) 3386.
[26] J. Eastoe, E.R. Crooks, A. Beeby, R.K. Heenan, Chem. Phys. Lett. 245 (1995) 571.
[27] I. Ramakanth, A. Patnaik, Carbon 46 (2008) 692.

[28] N. Gharbi, M. Pressac, M. Hadchouel, H. Szwarc, S.R. Wilson, F. Moussa, Nano Lett. 5 (2005) 2578.
[29] J.M. Treubig, P.R. Brown, J. Chromatogr. A 873 (2000) 257.
[30] M. Uchiama, M. Mihara, Anal. Biochem. 8 (1978) 271.
[31] G. Horvai (Ed.), Sokvaltozos Adatelemzes (Kemometria), Nemzeti Tankkonyvkiado, Budapest, Fejezet 1, 2001 (Hungarian Edition, text in Hungarian).
[32] Y. Tomioka, M. Ishibashi, H. Kajiyama, Y. Taniguchi, Langmuir 9 (1993) 32.
[33] I.C. Wang, L.A. Tai, D.D. Lee, P.P. Kanakamma, S. Clifton K.F., T.Y. Luh, J. Med. Chem. 42 (1999) 4614.
[34] L. Xiao, H. Takada, K. Maeda, M. Haramoto, N. Miwa, Biomed. Pharmacother. 59 (2005) 351.
[35] C. Tanford, The Hydrophobic Effect: Formation of Micelles and Biological Membranes, second ed., John Wiley & Sons Inc., New York, 1980.